Materials Science Forum
ISSN: 1662-9752, Vol. 1046, pp 45-58

Submitted: 2021-05-19
Revised: 2021-07-01
Accepted: 2021-07-07
Online: 2021-09-22

Behavior of CSC-Type Shear Connectors Under Pry-Out Shear Test: Analytical Study

X.F. Hurtado[1,a*] and M. Molina[2,b]

[1]Department of Civil and Agricultural Engineering. Universidad Nacional de Colombia. Department of Civil Engineering Universidad de La Salle. 111321 Bogotá, Colombia..

[2]Department of Civil and Agricultural Engineering. Universidad Nacional de Colombia. 111321 Bogotá, Colombia.

[a]xfhurtadoa@unal.edu.co, [b]mmolinah@unal.edu.co

Keywords: Cold-Formed steel, Shear connector, Pry-Out test, Finite element method, Composite section

Abstract. The use of cold-formed steel (CFS) shapes in steel-concrete composite sections has increased over the past 20 years in the construction industry worldwide. This system has constructive advantages such as high load-bearing capacity, high stiffness and ductility, ease of transportation and assembly, and full usage of the capacity of the materials. Additionally, CFS sections are considered a sustainable alternative in construction.
The capacity of the system depends on the effectiveness of shear connectors during the transfer of stress between materials. Currently, the push-out experimental test follows a standardized procedure to evaluate the capacity of shear connectors in composite sections, but CFS shapes have demonstrated premature failures by local buckling, thus questioning the applicability of the experimental test for such configurations.
In this research, the capacity of the proposed confined shear connectors (CSC) is evaluated in composite systems, through the alternative pry-out test methodology. From numerical models, the effects of the steel shape thickness, the thickness of concrete slabs, the compressive strength of concrete and the separation between connectors in composite systems are studied. The analysis concluded that, under this test methodology, the separation between connectors does not represent statistically significant changes in the final capacity of the composite system.

Introduction

Over the last 20 years, use of cold-formed steel (CFS) sections has increased considerably, particularly in medium and small structures [1] due to their multiple constructive advantages, such as high load-bearing capacity, high stiffness and ductility, and ease in transportation and installation, so it appears to be a cost-effective system. Furthermore, this typology of elements has been considered a sustainable alternative in the construction industry [2][3][4].

The application of CFS sections in composite floor systems with concrete slabs has emerged as an alternative to optimize the full use of materials and has been the focus of recent research. In this sense, it is necessary to verify the connection mechanism between the two materials to guarantee the stress transfer.

Currently, the design codes support four types of shear connectors as stress transfer elements: studs, channels, perfobond ribs, and screws [5][6][7][8][9][10]. These types of connectors were endorsed by experimental push-out tests on hot-rolled steel (HRS) sections, which have different mechanical properties concerning CFS sections, mainly regarding susceptibility to local buckling.

The traditional methodology to evaluate the capacity of shear connectors was proposed in the early 1950s by Viest et al. [11], Chinn [12], Slutter & Driscoll [13], Ollgard et al. [11], among others, who arranged the push-out experimental test. The experimental procedure is currently ruled in Eurocode 4 [9].

The experimental specimens are composed of two concrete slabs attached to a steel shape. The monotonic compression load is applied directly to the steel sections and transferred to the concrete slabs through the shear connectors (Fig 1). These connectors are generally welded to the steel plates.

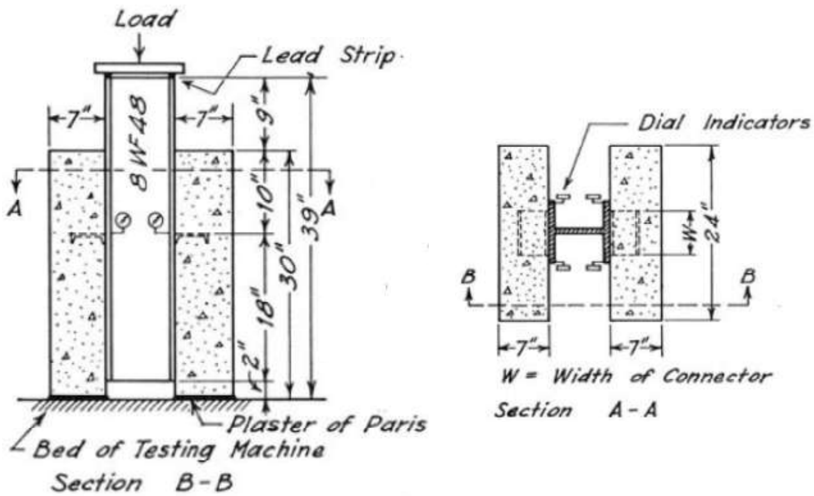

a) b)

Fig. 1 Details of push-out specimens: a) Front view and b) Cross section (taken from Viest et al. [11]).

Since CFS sections have limited thickness, this experimental test has proven to be inefficient to evaluate the full capacity of shear connectors in composite systems, causing early failures in plates due to local buckling. Therefore, the experimental data show low reliability. Local failures have been evidenced in the research of Lawan et al. [15][16][17], as shown in Figure 2.

a) b)

Fig. 2 Local buckling failure in push-out specimens: a) M16 bolt connectors and b) M14 bolt connectors (images taken from Lam et al. [15]).

As an alternative to this procedure, Anderson & Meinheit [16] proposed a particular methodology to evaluate the bearing capacity of shear connectors as transfer elements, called the pry-out test. In this arrangement, there is only one concrete slab and the steel section is loaded under tensile loadcondition. Therefore, the system failure can be caused by issues with the steel section, the concrete, the shear connectors, or a combination of these (Fig 3). According to current design codes, any type of shear connector different from the endorsed ones must be validated through a series of experimental tests.

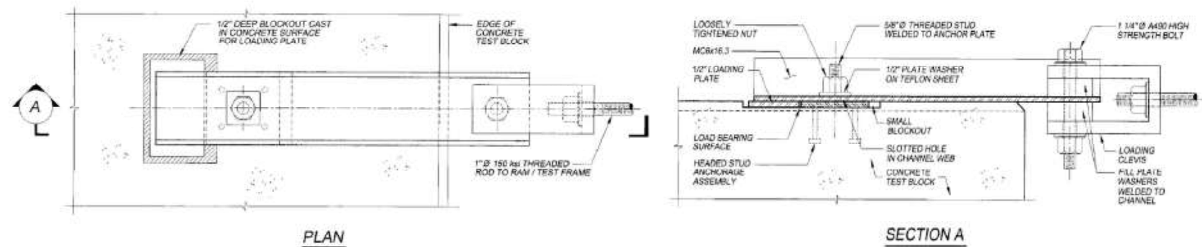

a) b)

Fig. 3 Setup of pry-out test: a) Plan view and b) longitudinal section (images taken from Anderson & Meinheit [16]).

In this research, an analytical study is carried out and a new typology of shear connectors is proposed, called CSC (confined shear connectors) [19]. Self-drilling screws are simulated as a fixing mechanism for the connectors, thus avoiding the disadvantages of welding, such as residual stresses or perforations in steel plates due to burns [20]. Numerical models were developed using the finite element method (FEM) in ANSYS software. Then, the incidence of the thickness of the concrete slab, the thickness of steel section, the spacing between connectors and the compressive strength of concrete were validated in the whole bearing system, through pry-out test simulations. Analytical procedures can predict non-linear responses and ultimate load capacities as an alternative to such an expensive experimental test [21][22].

A central composite face-centered (CCF) statistical design [23] was arranged to assess the most representative analysis of geometrical variable configurations in analytical models, concluding that spacing does not significantly affect the load transfer capacity of the connectors under this type of test.

Description of Models

Description of specimens. ANSYS Workbench was the software selected to simulate the mechanical behavior of the specimens. All components were modeled using 3D quadratic elements for more accurate results.

All of the analytical models developed were composed of shear connectors and reinforcement bars embedded into a 700mm x 200mm x 100/140mm concrete slab (Fig 4). The structural model included 6mm-diameter self-drilling screws and 700mm-long steel sections. The internal elements were removed from the concrete block and replaced by steel pieces.

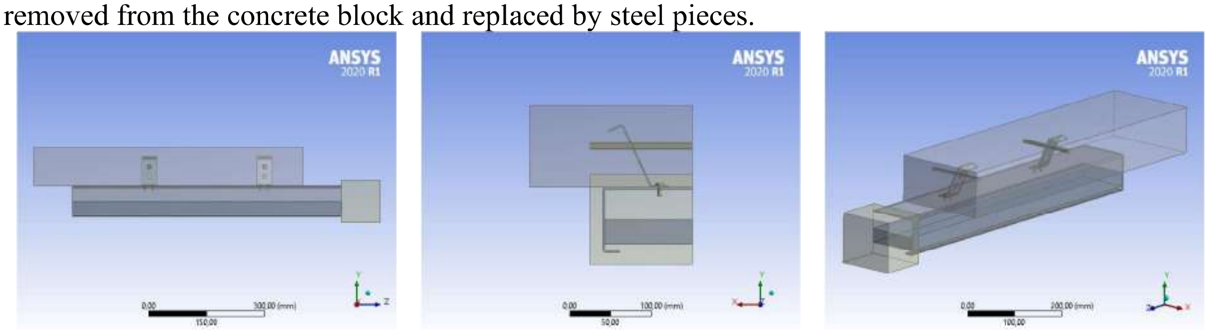

a) b) c)

Fig. 4 Structural simulation model: a) Side view, b) front view and c) 3D view.

All the arrangements of the specimens are listed in Table 1. The variables considered in this research were the thickness of concrete slab, the thickness of steel section, the nominal compressive strength of concrete, and the spacing between connectors.

Table 1 Description of study variables and levels.

N°	Specimen	Compressive strength of concrete (A)	Thickness of steel section (B)	Thickness of concrete slab (Block)	Spacing between connectors (C)
		[MPa]	[mm]	[mm]	[mm]
1	PO 2-21-100@200	21	2	100	200
2	PO 2-21-100@400	21	2	100	400
3	PO 2-35-100@200	35	2	100	200
4	PO 2-35-100@400	35	2	100	400
5	PO 2.5-28-100@300	28	2.5	100	300
6	PO 3-21-100@200	21	3	100	200
7	PO 3-21-100@400	21	3	100	400
8	PO 3-35-100@200	35	3	100	200
9	PO 3-35-100@400	35	3	100	400
10	PO 2-28-140@300	28	2	140	300
11	PO 2.5-21-140@300	21	2.5	140	300
12	PO 2.5-28-140@200	28	2.5	140	200
13	PO 2.5-28-140@300	28	2.5	140	300
14	PO 2.5-28-140@400	28	2.5	140	400
15	PO 2.5-35-140@300	35	2.5	140	300
16	PO 3-28-140@300	28	3	140	300

Materials. The material properties of the components of the finite element models were represented by constitutive laws and their nominal properties.

Concrete.

The non-linear behavior of concrete was characterized as multi-linear isotropic hardening by an equivalent uniaxial stress-strain curve (Fig 5a), which uses Von Misses yield criterion. The relationship between compression stress and the strain was obtained from Eq. (1) and Eq. (2). The compression was assumed to be linear elastic up to 0.40 f'_c. The negative gradient in the last stage of the stress-strain curve was not considered.

$$\sigma_c = \frac{f'_c \gamma \left({\varepsilon_c}/{\varepsilon'_c} \right)}{\left[\gamma - 1 + \left({\varepsilon_c}/{\varepsilon'_c} \right)^{\gamma} \right]} \tag{1}$$

$$\gamma = \left(\frac{f'_c}{32.4} \right) + 1.55 \tag{2}$$

where f'_c is the nominal compressive strength of concrete, σ_c is the uniaxial compression stress and ε_c is the uniaxial strain of the concrete. The term ε'_c is the maximum strain at the maximum stress and is defined as 0,0025.

Steel. For all the elements, steel material was modeled as elastoplastic using the bilinear curve, as shown in Figure 5b. Small hardening was applied to achieve convergence. Nominal properties are presented in Table 2.

Table 2 Nominal mechanical properties of steel components.

		Shear connector (ASTM A424 - Type II)	Self-drilling screw fastener (ASTM A449)	Steel reinforcement (ASTM A706)	Steel section (ASTM A1011)
		[MPa]	[MPa]	[MPa]	[MPa]
Modulus of elasticity	(Es)	200.000	200.000	200.000	200.000
Yield stress	(fy)	240	644	420	350
Ultimate tensile stress	(fu)	350	840	560	420

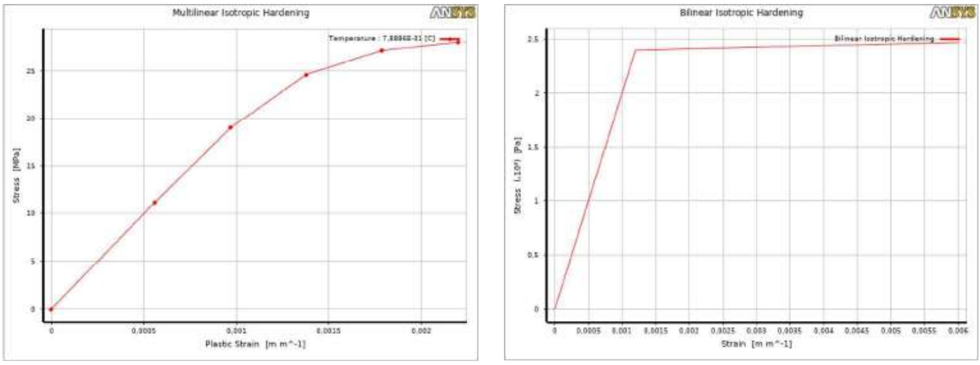

a) b)

Fig. 5 Uniaxial stress-strain relationship for different materials: a) Concrete and b) steel.

Interaction and boundary conditions. Due to the symmetry of the specimens, only half of the system was modeled in the analysis in order to reduce the simulation time. Therefore, all nodes along the symmetry plane of the concrete slab, steel section and reinforcing bar were restricted from moving in the X direction (Fig 6a).

Only a side face of the concrete slab was considered as fixed support, thus all degrees of freedom (DOFs) were restricted. Moreover, all nodes on the upper face had restricted movement in the Y direction, in order to avoid uplifts and rotations in the specimen because of eccentricity in the load (Fig 6a).

The monotonic load was applied as enforced lateral displacement on the concrete slab in the Z direction through a steel block, in order to simulate experimental conditions. An additional element was included along the steel section, which restrains deformations in the flanges. Due to the limited movements in the system, large displacements were not considered (Fig 6a).

Interaction between different elements was modeled by using both frictionless and frictional contacts to represent the behavior of the surfaces in the specimen components, avoiding free sliding and focusing on the mechanical restriction generated within the concrete slab. The value for the friction coefficient was assumed to be 0.80 between fasteners and shear connectors, and fasteners and steel section, due to the high connection evidenced in previous experimental tests [20] (Fig 6b).

The unsymmetric Newton-Raphson method was applied to solve non-linear equations according to the user guide of the ANSYS manual. The software performs an iterative approach to obtain equilibrium in each increment in displacement.

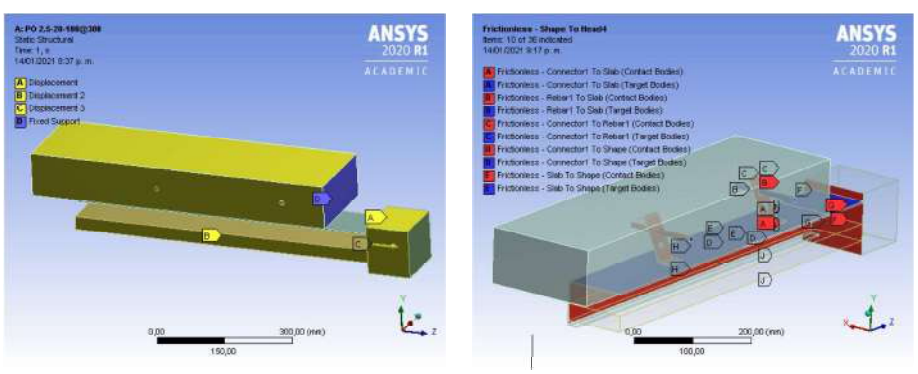

a) b)

Fig. 6 Modeled system: (a) Boundary conditions in the whole specimen and (b) contact interaction between different elements.

Meshing. The discretization of each element of the model was made by applying a coarse adaptive mesh. The fine mesh was applied at the connector, the reinforcing bar, and the fasteners areas to obtain more accurate results. The overall mesh size was around 50mm and it was reduced to 2mm on contact surfaces, where a high gradient was expected (Fig 7).

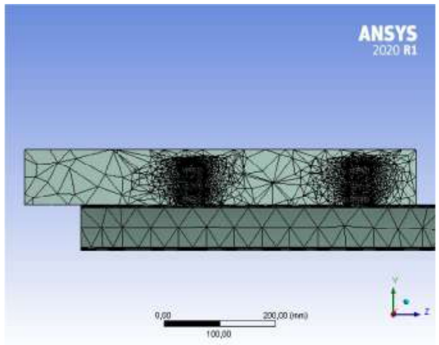

a)

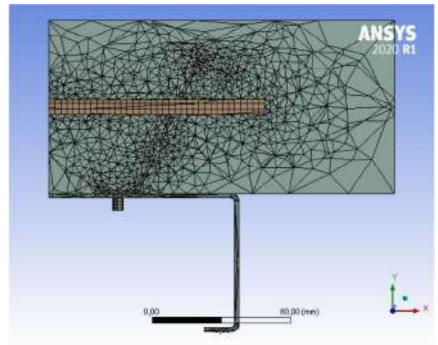

b)

Fig. 7 Specimen mesh model: (a) Side view and (b) cross section.

Results

Displacements. The displacement is applied to the steel section and transferred as load to the concrete slab through the shear connectors. Fig 8 presents the general displacements of the system.

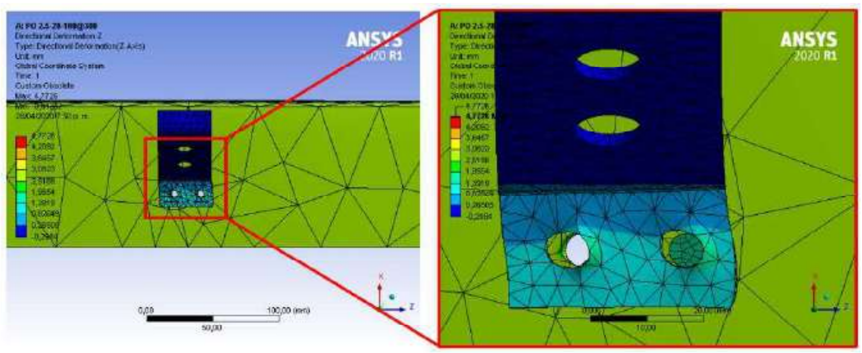

a)

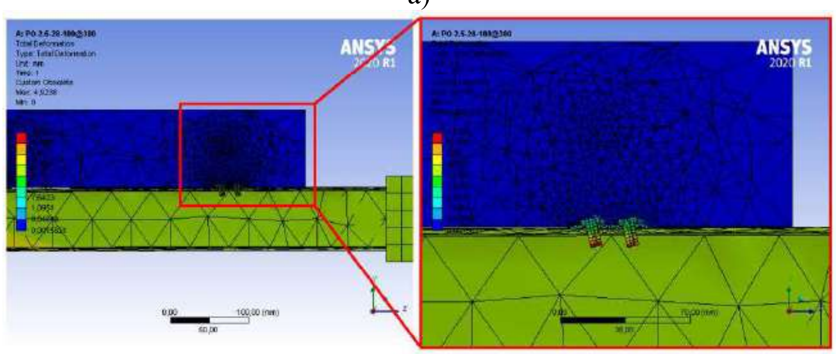

b)

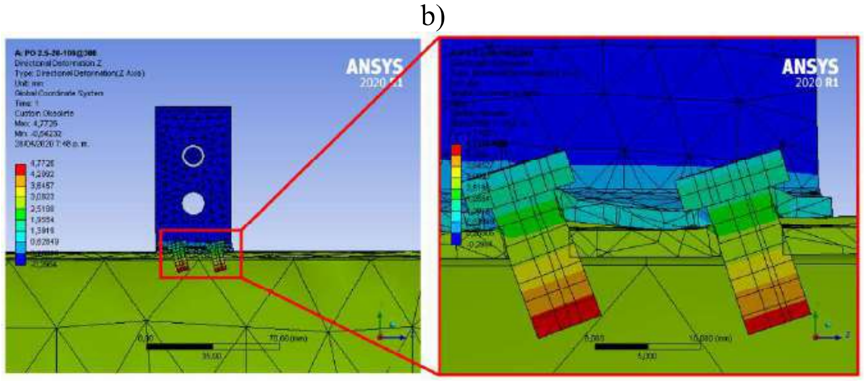

c)

Fig. 8 Displacement in Z-direction: Local views of a) steel elements, b) concrete slab and c) fastening system.

Due to the difference in stiffness between the elements and the fastening system, the connector and steel shape plates have greater local deformations (Fig 8a) with respect to the concrete slab, where the deformation is minimal (Fig 8b). In this way, rotations on the screws were induced (Fig 8c). This final condition was evident in all numerical models.

The displacements in the steel sections are shown in Fig 9. According to the non-uniform distribution along with the element, it is concluded that the specimen does not behave as a rigid body due to the limited thickness of the steel plates (Fig 9c). Fig 9a shows an increase in X-direction displacements in the middle steel section, which are conditioned by the inclusion of an additional element proposed for experimental tests. Additionally, possible uplifts during the experimental test (Fig 9b) should be controlled and restricted by setup accessories.

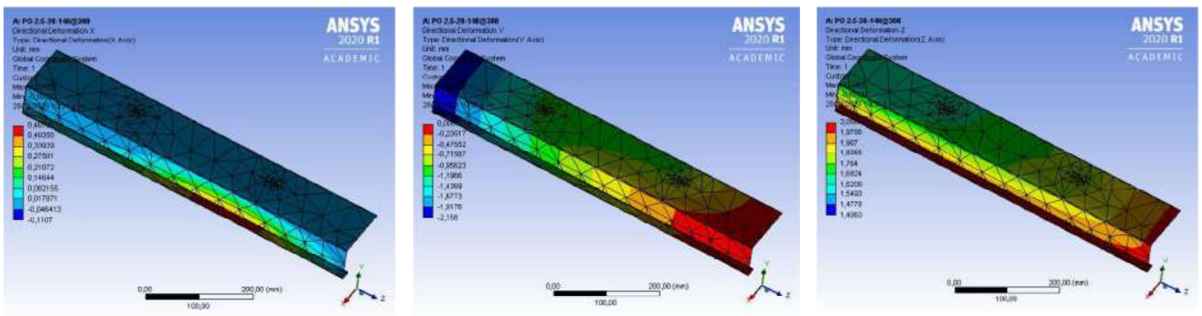

a) b) c)

Fig. 9 Displacements in steel section: a) X direction, b) Y direction and c) Z direction.

Stress. According to the process of load evolution, the participation of all the connection elements of the system is perceived, allowing transferring stresses from the steel section to the concrete slab. In this sense, the full interaction between elements of the composite section is achieved.

Self-drilling screws are the primary elements of stress transmission between the steel section and the shear connectors. The connectors mechanically transfer the forces to the concrete slab, due to their geometry and the concrete dowel produced in the lower perforation. Likewise, the rebar receives the forces from the connectors and spreads them in a larger concrete area, thus avoiding concentrations of stress and early cracking in the concrete slab. Consequently, this configuration allows increasing the load capacity of the system.

The failure mechanism starts with cracking in the concrete slab around the connector, mainly in the compression affectation area. Subsequently, plastification in shear connectors occurs, beginning in the lowest fold of the element (Fig 10a and b). Fig 10c shows the final stress state of the concrete, and Fig 10d includes the interaction of all the components in the transfer zone.

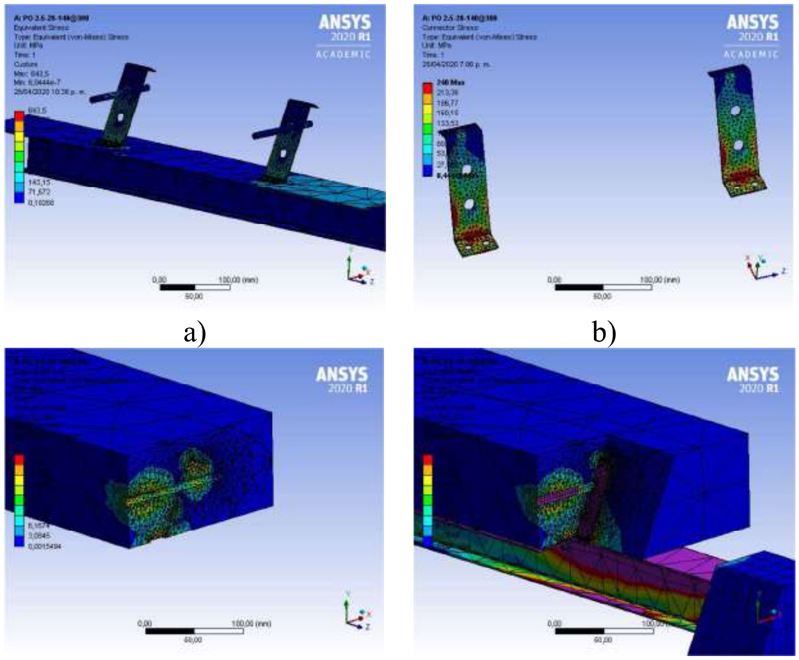

a) b)

c) d)

Fig. 10 Final stress state in specimens: a) Steel components, b) shear connectors, c) concrete slab detail and d) local view of the whole specimen.

Discussion

Load-displacement curves. According to the experimental methodology included in Eurocode 4 [9] and other reference research [11][12][13][14], the complete record of load and displacement data was considered (Fig 11a). In Fig 11b, data logging is restricted to the maximum elastic behavior capacity in the connectors, before starting the steel plastification as part of the failure mechanism of the system.

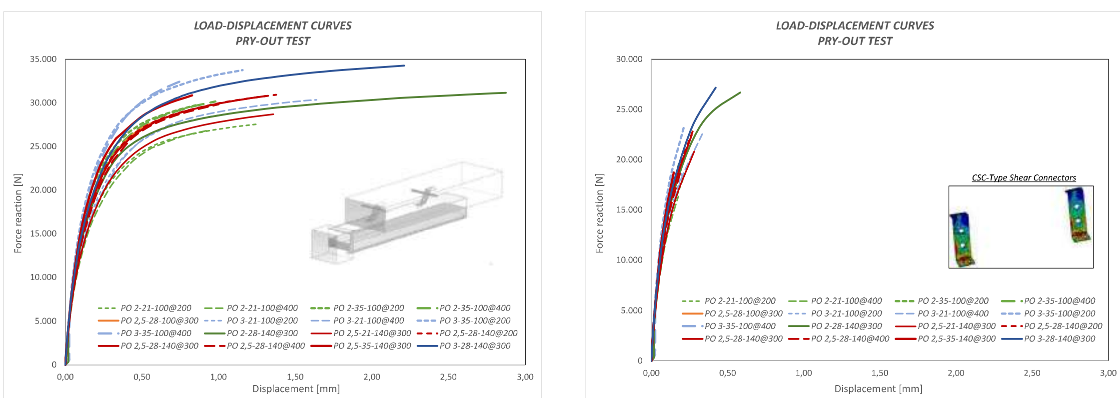

a) b)

Fig. 11 Reaction load vs. displacement curves: a) Full data logging and b) Data logging during elastic behavior of shear connectors.

The tendency of the curves shows the nonlinear behavior of the system, with the progressive degradation of its stiffness once the maximum compression strength of concrete is reached. Although connectors present plastification in all specimens, these two failure conditions do not occur simultaneously.

According to the limits of the variable established in this research, the maximum load values are between 27000N and 34000N, and maximum displacements are close to 3mm in a 140mm-thick concrete slab. In general, the maximum displacements were in the range of 1.0mm to 1.5mm. Table

3 shows the log summary data. The elastic behavior is around 20% of the maximum state of displacement, and between 60% and 70% of the maximum state of the load.

Table 3 Summary data.

N°	Specimen	Elastic Reaction Force	Elastic. Displacement	Max. Reaction Force	Max. Displacement	Forces ratio	Displac. ratio
		[N]	[mm]	[N]	[mm]	[%]	[%]
1	PO 2-21-100@200	19389	0.24	27562	1.25	70.3	19.1
2	PO 2-21-100@400	16323	0.17	26865	0.94	60.8	18.6
3	PO 2-35-100@200	18727	0.15	29710	0.85	63.0	17.2
4	PO 2-35-100@400	19537	0.18	30173	0.98	64.7	18.3
5	PO 2,5-28-100@300	17268	0.15	28973	0.77	59.6	19.0
6	PO 3-21-100@200	18591	0.20	28799	1.08	64.6	18.5
7	PO 3-21-100@400	22542	0.33	30355	1.64	74.3	20.3
8	PO 3-35-100@200	23322	0.21	33771	1.16	69.1	18.4
9	PO 3-35-100@400	18974	0.15	32607	0.77	58.2	18.9
10	PO 2-28-140@300	26701	0.58	31152	2.87	85.7	20.3
11	PO 2,5-21-140@300	20829	0.28	28693	1.36	72.6	20.7
12	PO 2,5-28-140@200	22896	0.27	30930	1.38	74.0	19.8
13	PO 2,5-28-140@300	22439	0.26	30797	1.31	72.9	20.1
14	PO 2,5-28-140@400	19059	0.19	29820	1.00	63.9	19.3
15	PO 2,5-35-140@300	18717	0.15	30855	0.83	60.7	17.8
16	PO 3-28-140@300	27164	0.42	34252	2.21	79.3	19.0

As only a half section of each specimen was modeled, the maximum system loads shown here should be duplicated. As established in Eurocode 4 [9], connectors that present less than 6mm displacements are taken as rigid connectors, such as CSC shear connectors.

Statistical analysis. The statistical analysis aims to evaluate the incidence of the variables involved in this study on the behavior and final capacity of the system: (A) Compressive strength of concrete, (B) thickness of steel section, (C) spacing between connectors, and (block) thickness of concrete slab (Table 1). In the randomized block design (RBD) [23], the block represents a variable that needs to be analyzed independently at each level under study, due to the particularity of its configuration. In this case, the change in the thickness of the concrete slab involves geometric modifications of the connector and the arrangement of elements. Fig 12 shows the variable interaction plot.

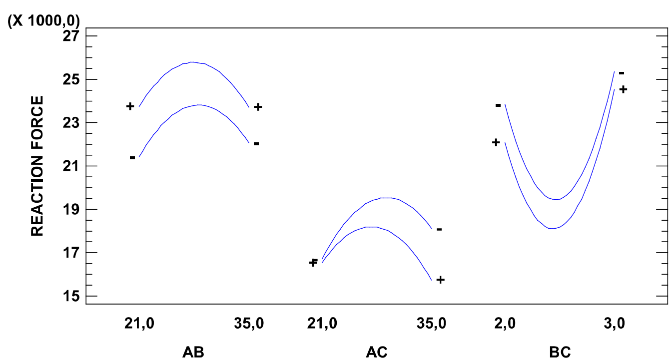

Fig. 12 Interaction plot.

Since there is no point of intersection in the curves, there is no interaction of variables within the range of values under study. Therefore, the effect of each factor can be studied independently of the overall behavior of the system.

One-way analysis of variance (ANOVA) allows carrying out this statistical evaluation by comparing response means in multiple ranges. In this case, Fisher's LSD procedure was used to examine the possible overlaps in confidence intervals (Fig 13).

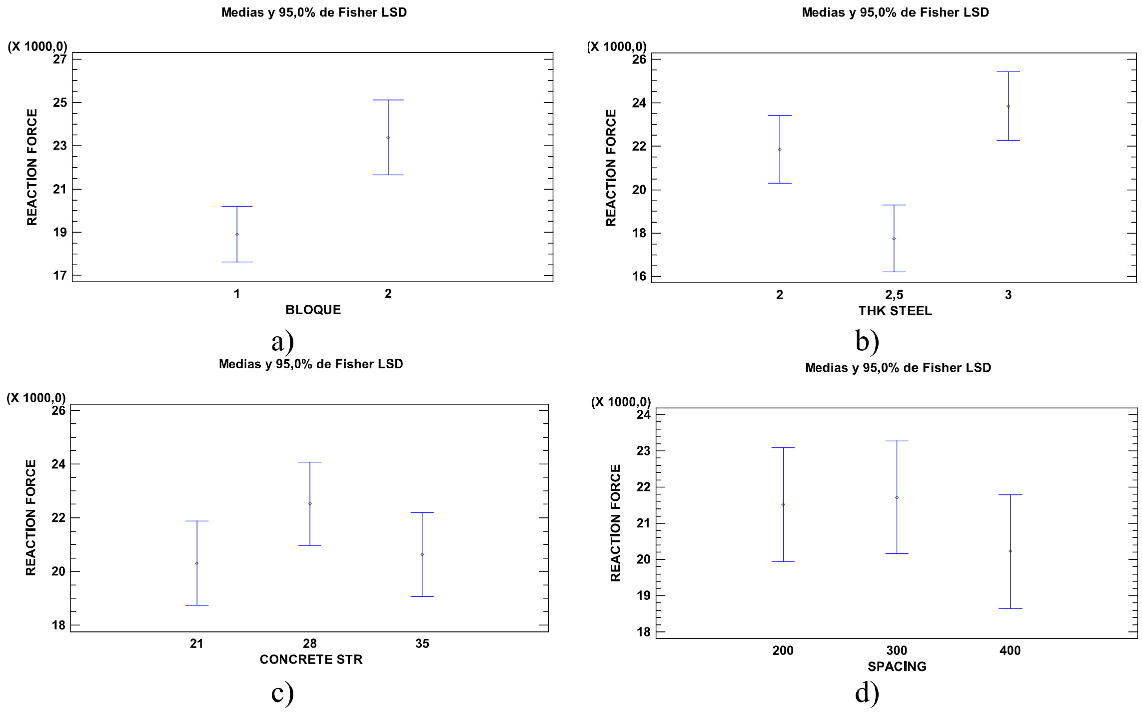

Fig. 13 Means plots: a) Thickness of concrete slab, b) thickness of steel section, c) compressive strength of concrete and d) spacing between connectors.

As mentioned previously, the block assigned by the difference in thickness in the concrete slabs shows statistically different behaviors at 100mm and 140mm (Fig 13 a.). Likewise, the response of the system varies with respect to the thickness of the steel shape, thus reducing the final load in specimens with 2.5mm-thickness sections. In contrast, for the other thicknesses, the maximum values remain within the same magnitude range (Fig 13b).

Although there are slight variations within the range of responses, it is concluded that the contribution of the nominal compressive strength of concrete to the capacity of the system is low with respect to the variables indicated before, even considering the possibility of statistical equality (Fig 13c).

Regarding spacing, the response indicates that the variation of the parameter is not statistically significant in the final capacity of the system, and can be omitted from the analysis (Fig 13d). This result must be statistically validated with the response of the experimental tests.

According to the results, the response surfaces shown in Fig 14 are generated and the variation of the maximum elastic load states are presented with respect to the evolution of the different levels of the variables under study.

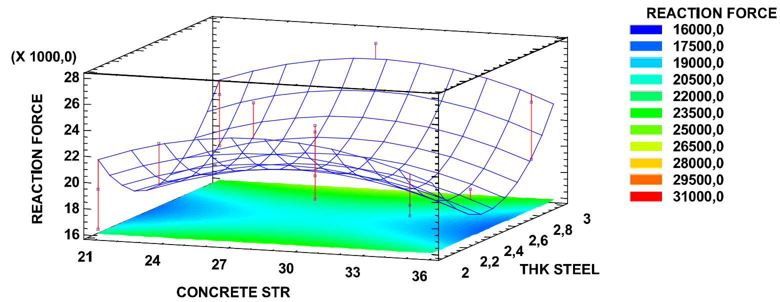

a).

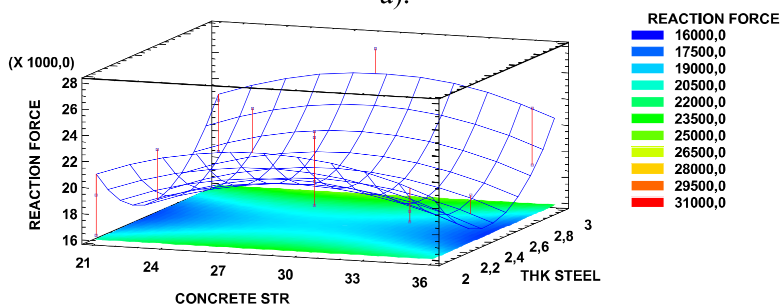

b).

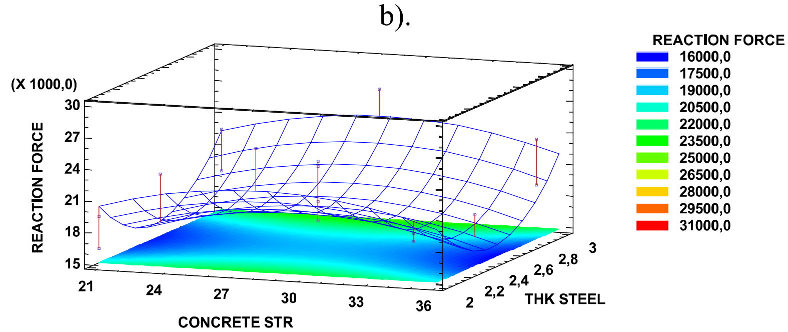

c).

Fig. 14 Response surfaces for the studied spacing: a) 200mm, b) 300mm and c) 400mm.

Parametric studies. In the parametric analysis, it was possible to compare the final stress state of the different components of the system based on their different geometric and mechanical variables.

Effect of thickness of steel section. Unlike shear connectors, the final stress state in steel shapes does not reach the complete plastification of the section. Instead, there are local stress concentrations in the connection area with the self-drilling screws. According to the thicknesses studied, in 2mm-thickness sections, the stress distribution extends to a larger area. As the thickness increases (2.5mm and 3mm), the area of influence is reduced and there is greater uniformity in the maximum stress value (Fig 15).

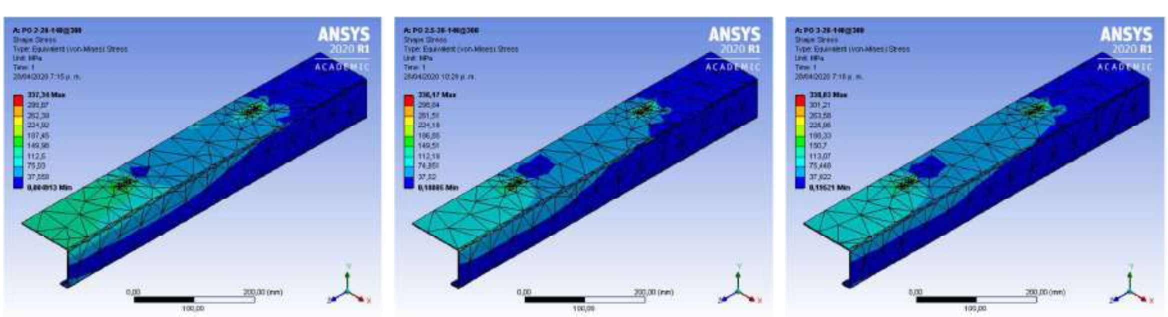

a) b) c)

Fig. 15 Final stress state in steel section: a) 2mm-thickness, b) 2.5mm-thickness and c) 3mm-thickness.

Effect of thickness of concrete slab. This study evaluated concrete slabs of 100mm and 140mm-thickness. As shown in Figure 16, in both cases the maximum compressive strength of concrete was reached locally, around the connectors and rebar, due to the induced crushing after the application of the load. Due to the type of contacts used in the modeling, free displacements between steel and concrete elements were enabled, thus omitting the contribution of friction in the system, allowing the evaluation of the net capacity of the mechanical anchor given by the geometry of the connector and minimizing stresses in the concrete. The maximum load capacity was higher in the thickest slab.

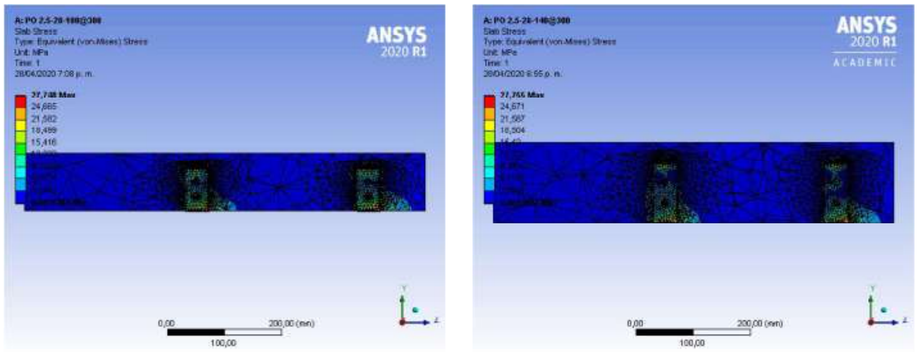

a) b)

Fig. 16 Final stress state in concrete slab: a) 100mm-thick specimen, b) 140mm-thick specimen.

Effect of compressive strength of concrete. The degradation process of the system begins in the concrete due to the local crushing around the connector and the reinforcement bar. The affected area is larger in lower-strength concrete (Fig 17). Although the variation in concrete strength causes slight differences in the final response of the system, this effect is not as representative as other variables.

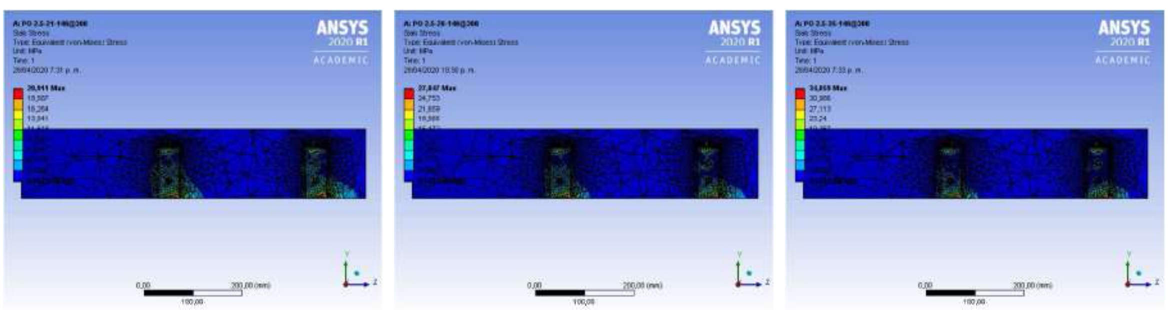

a) b) c)

Fig. 17 Final stress state in concrete slab of: a) 21MPa-strength, b) 28MPa-strength and c) 35MPa-strength.

Effect of spacing between connectors. As discussed in the statistical analysis, the spacing between connectors has no statistically significant variation under the pry-out test methodology. Fig 18 shows the different stress states of the system for 200mm, 300mm, and 400mm spacing. In this way, both the connectors and the concrete slab show a similar behavior in the three configurations. It is evident that the load distribution is not uniform in the connectors, due to the proximity of one of them to the point of load application.

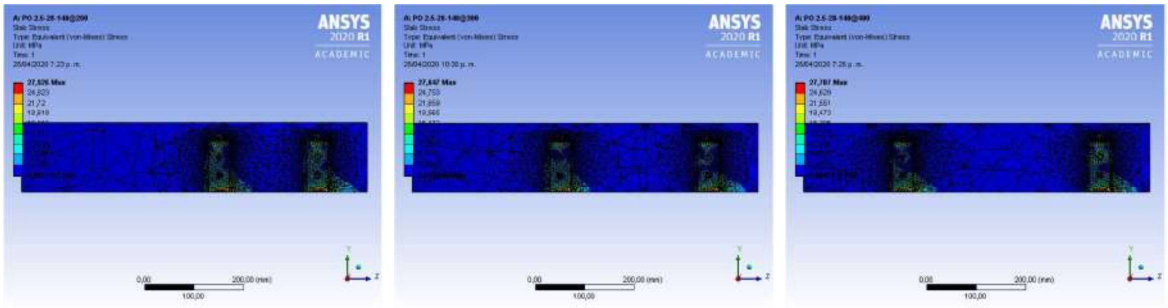

a) b) c)

Fig. 18 Final stress state in specimens with spacing of: a) 200mm, b) 300mm and c) 400mm.

Conclusions

This paper presents the results of the pry-out numerical test models. This alternative test serves to evaluate the capacity of composite sections using cold-formed steel (CFS) sections and CSC-type shear connectors in order to reduce the possibility of local buckling failures, as evidenced in the traditional push-out experimental test. The steel section shows non-uniform displacements during the loading process. Therefore, this type of section does not work as a rigid body due to the thickness of the plates.

The modeling results allow identifying the initiation of the crush failure mechanism in the concrete slab, around the connectors, and rebar. Subsequently, the CSC-type shear connectors start the plastification process in the lower fold that spread throughout the element until the system is unstable.

Under this type of test, the compressive strength of concrete and mainly the separation between connectors proved to have a low impact on the capacity of the system from a statistical point of view. In this sense, the separation could be excluded as an analysis variable. It is recommended that qualitative and quantitative results be validated by conducting pry-out experimental tests.

References

[1] S.O. Bamaga, M.M. Tahir, & C.S. Tan, Push tests on innovative shear connector for composite beam with cold-formed steel section, in: International Specialty Conference on Cold-Formed Steel Structures, Scholars' Mine, USA Missouri University of Science and Technology, St. Louis, 2012.

[2] T.M. Alhajri, M.M. Tahir, M. Azimi, J. Mirza, M.M. Lawan, K.K. Alenezi, & M.B. Ragaee, Behavior of pre-cast u-shaped composite beam integrating cold-formed steel with ferro-cement slab, Thin-Walled Structures 102 (2016) 18-29.

[3] J.M. Irvwan, A.H. Hanizah, & I. Azmi, Test of shear transfer enhancement in symmetric cold-formed steel concrete composite beams, J. Const. Steel Res. 65 (2009) 2087-2098.

[4] M.M. Lawan, M.M. Tahir, S.P. Ngian, & A. Sulaiman, Structural performance of cold-formed steel section in composite structures: a review. Jurnal Teknologi 74 (4) (2015) 165-175.

[5] ANSI/AISC 360-16: Specification for Structural Steel Buildings, American Institute of Steel Construction, Chicago, 2016.

[6] ABNT 8800: Norma Brasileira – Projeto de Estruturas de Aço e de Estruturas Mistas de Aço e Concreto de Edificios, Associação Brasileira de Normas Técnicas, Rio de Janeiro, 2008.

[7] AS/NZ 4600:2005: Cold Formed Steel Structures, Australian/New Zeland Standards, Sydney, 2005.

[8] NSR10. Norma Colombiana de Diseño y Construcción Sismo Resistente. Asociación de Ingeniería Sísmica. Bogotá, 2010

[9] BS EN 1994-1-1: Eurocode 4, Design of Composite Steel and Concrete Structures: Part 1-1, General Rules and Rules for Buildings, British Standard Institution London, 2004.

[10] Standard Specifications for Steel and Composite Structures – III Design, Japan Society of Civil Engineers (JSCE), Tokyo, 2007.

[11] Viest, I. M., Siess, C. P., Appleton, J. H. & Newmark N. M. Full-Scaled test of channel shear connectors and composite T-beams. Report of investigation. University of Illinois Bulletin N° 405. 1952.

[12] Chinn, J. Push-out tests on lightweight composite slabs. Engineering Journal, AISC. (1965) 129-134.

[13] Slutter, R., & Driscoll, G. Flexural strength of steel and concrete composite beams. Final report of an investigation of composite beams for buildings sponsored by the American Institute of Steel Construction (1963) 1-57.

[14] Ollgaard, J., Slutter, R., & Fisher, J. Shear strength of stud connectors in lightweight and normal-weight concrete. AISC Engineering Journal (1971) 55-64.

[15] Lawan, M., Tahir, M., & Mirza, J. Bolted shear connectors performance in self-compacting concrete integrated with cold-formed steel section. Latin American Journal of Solids and Structures, 13(4), 2016) 731–749.

[16] Lawan, M., Tahir, M., & Osman, M. Composite construction of cold-formed steel (cfs) section with high strength bolted shear connector. Jurnal Teknologi, 77(16) (2015) 171–179.

[17] Lawan, M., Tahir, M., & Hosseinpour, E. Feasibility of using bolted shear connector with cold-formed steel in composite construction. Jurnal Teknologi, 78(6–12) (2016) 7–13.

[18] Anderson, N & Meinheit, D. Design criteria for headed stud groups in shear. PCI Journal (2000). 46-75.

[19] Hurtado, X. & Molina, M. Geometrical and mechanical optimization of shear connectors fod CFS-concrete composite systems. The 2020 Structures Congress (2020) 25-28.

[20] Hurtado, X.F. & Molina, M. Alternative fastening mechanism for shear connectors with cold-formed steel shapes involved in composite sections, Athens Journal of Technology and Engineering 7(2) (2020) 133-156.

[21] Titoum, M., Mazoz, A., Benanane, A. & Ouinas, D. Experimental study and finite element modelling of push-out test on a new shear connector of i-shape. Advanced Steel Construction, Vol. 12, N° 4, (2016) 487-506.

[22] Raj, P. V. & Sathiya B. P. An analytical and experimental investigation of shear connectors in composite sections. International Research Journal of Engineering and Technology (IRJET). Vol 04, N° 6 (2017) 991-999.

[23] D. Montgomery, Design and Analysis of Experiments, eighth ed., Wiley, New Jesey, 2013.